

## InterPACK2013-73128

### EFFECT OF FIN INTERRUPTIONS ON NATURAL CONVECTION HEAT TRANSFER FROM A RECTANGULAR INTERRUPTED SINGLE-WALL

**Golnoosh Mostafavi**

Laboratory for Alternative Energy Conversion  
(LAEC), Mechatronics System Engineering, SFU  
Surrey, British Columbia, Canada

**Mehran Ahmadi**

Laboratory for Alternative Energy Conversion  
(LAEC), Mechatronics System Engineering, SFU  
Surrey, British Columbia, Canada

**Majid Bahrami**

Laboratory for Alternative Energy Conversion  
(LAEC), Mechatronics System Engineering, SFU  
Surrey, British Columbia, Canada

#### ABSTRACT

Steady-state external natural convective heat transfer from a single-wall vertically-mounted rectangular interrupted fin arrays is investigated. A systematic numerical, experimental, and analytical study is conducted on the effect of adding interruptions to a single vertical plate, on natural convective heat transfer. COMSOL Multiphysics software is used in order to develop a two-dimensional numerical model for investigation of fin interruption effects. To perform an experimental study and to verify the analytical and numerical results, a custom-designed testbed was developed. Results show that adding interruptions to a vertical single fin enhances the thermal performance of it and reduces the weight of the heatsink, which in turn, can lead to lower manufacturing costs. A compact relationship for the Nusselt number based on geometrical parameters for interrupted fins is presented using a blending technique for two asymptotes of interruption length.

#### 1. INTRODUCTION

The design of efficient cooling system is essential for reliable performance of high power density electronics. Generally 55% of failure mechanisms in electronic devices are related to thermal effects. In fact, the rate of such failures nearly doubles with every 10°C increase above the operating temperature (~80°C) of high power electronics [1]. With the current trend in industry, as the power density of electronics is increasing and their sizes are decreasing at the same time, heatsinks have to be able to dissipate higher heat fluxes.

Therefore, devising efficient cooling solutions to meet these challenges is of paramount importance and has direct impacts on the performance and reliability of electronic and power electronic devices.

Passive cooling methods are widely preferred for electronic and power electronic devices since they provide low-price, noiseless, and trouble free solutions. Air-cooling also is recognized as an important technique in the thermal design of electronic packages, because besides its availability, it is safe, does not contaminate the air and does not add vibrations, noise and humidity to the system in which it is used [2]. Such features of natural convection stimulated considerable research on the development of optimized finned heatsinks and enclosures [3, 4, 5].

The focus of this study is on natural convective heat transfer from interrupted, vertical and rectangular single fin arrays. However, a more general overview on pertinent literature in the area of natural heat transfer from fins is provided in this section. A variety of theoretical expressions, graphical correlations and empirical equations have been developed to represent the coefficients for natural convective heat transfer from vertical plates. Ostrach [6] made an important contribution on analysing the natural convective heat transfer from vertical fins. He analytically solved laminar boundary layer equations through similarity methods for uniform fin temperature condition and developed a relationship for the Nusselt number for different values of Prandtl number. As well, Sparrow and Gregg [7] used similarity solutions for boundary layer equations for the cases of uniform surface heat flux. Churchill and Chu [8] also developed an expression for Nusselt number for all ranges of the Ra, and Pr numbers. As it

can be seen, the main focus of the pertinent research in the area of the natural convective heat transfer from fins has been mostly on continuous fins and pin fins, and no in-depth study has been performed to investigate the natural convective heat transfer from interrupted fins for external natural convective heat transfer. Interrupted fins have been mostly studied for internal natural convection [9], [10] and forced convection, as in [11]. The present study aims to address this shortcoming by investigating the effect of fin interruption on the efficiency with which the heat is transferred from the heatsink to the environment. Figure 1 shows a schematic of the interrupted fin array investigated in this study. All the important geometrical parameters are also shown in the figure.

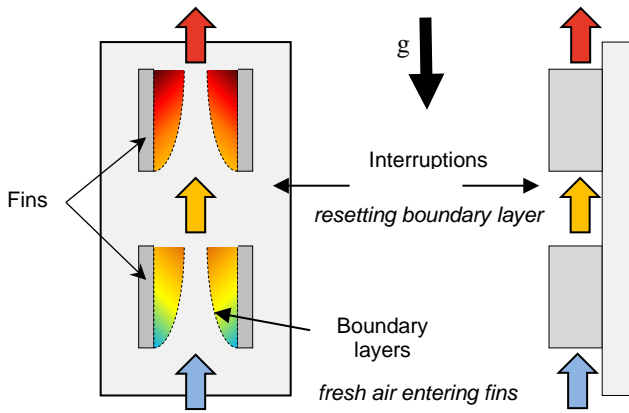


**Figure 1: Effect of adding interruptions on the boundary layer growth in natural heat transfer from vertical fins.**

As it can be seen in Fig. 1, interrupted fins are a more general form of fins and can include both continuous and pin fins at the limit where the fin interruption length approaches zero and infinity respectively. In other words, continuous fins and pin fins are two extreme cases of the targeted interrupted fins. The analysis was started expecting that a proper selection of fin spacing and interruption sizes can lead to a higher thermal performance. This expectation was based on the fact that interrupted fins exhibit a thermal boundary layer interruption, which help increase the heat flux [12]. Additionally, fin interruption leads to significant weight reduction, which in turn, can lower the manufacturing costs. As results, the goal of this study is to investigate the effects of adding interruptions to fins. The focus will be mainly on the fin length and interruption length. Also, in order to study the natural convective heat transfer from interrupted fins, a new concept, effective length, is introduced and a new relationship for the Nusselt number is developed based on non-dimensional geometrical parameters.

## 2. NUMERICAL ANALYSIS

### 2-1 GOVERNING EQUATION

We seek a solution for steady-state laminar natural convective heat transfer from an interrupted vertical fin array (Fig. 1). The conservation of mass, momentum and energy in the domain are based on assuming a fluid with constant properties and the Boussinesq approximation [13] for density-temperature relation:

$$\frac{\partial u}{\partial x} + \frac{\partial v}{\partial y} = 0 \quad (1)$$

$$\rho \left( u \frac{\partial u}{\partial x} + v \frac{\partial u}{\partial y} \right) = -\frac{\partial P}{\partial x} + \mu \nabla^2 u \quad (1)$$

$$\rho \left( u \frac{\partial v}{\partial x} + v \frac{\partial v}{\partial y} \right) = -\frac{\partial P}{\partial y} + \mu \nabla^2 v - \rho g \quad (2)$$

$$\left( u \frac{\partial T}{\partial x} + v \frac{\partial T}{\partial y} \right) = \alpha \nabla^2 T, \quad (3)$$

where  $y$  is the direction parallel to the gravitational acceleration and  $x$  is the direction normal to the gravitational acceleration,  $u$  is the flow velocity in  $x$ -direction and  $v$  is the flow velocity in  $y$ -direction, respectively.  $\rho$ ,  $\mu$  and  $\alpha$  are the fluid's density, dynamic viscosity and thermal diffusivity, respectively.

Considering  $\frac{\partial P}{\partial y} = \frac{\partial P_\infty}{\partial y}$ , where  $P_\infty$  is the ambient hydrostatic pressure, and assuming Boussinesq approximation, Eq. 3 yields to:

$$\rho \left( u \frac{\partial v}{\partial x} + v \frac{\partial v}{\partial y} \right) = \mu \nabla^2 v - g \beta \rho_\infty (T - T_\infty) \quad (5)$$

where in our numerical simulation in COMSOL the term,  $-g \beta (T - T_\infty)$ , is inserted to the equations as a body force.

Inlet boundary condition is applied to the bottom of the domain which defines the boundary condition for the velocity at the inlet. As such, we assumed gauge pressure to be zero. For the top and sides of the domain, an outlet boundary condition is applied. For the interruption region, the symmetry boundary condition was chosen. This type of boundary condition is equivalent to a no-heat flux in the direction normal to the plane. A no-slip isothermal solid surface is considered for the walls. Figure 2 shows a schematic of the domain considered for the numerical simulation, along with the chosen boundary conditions for fins.

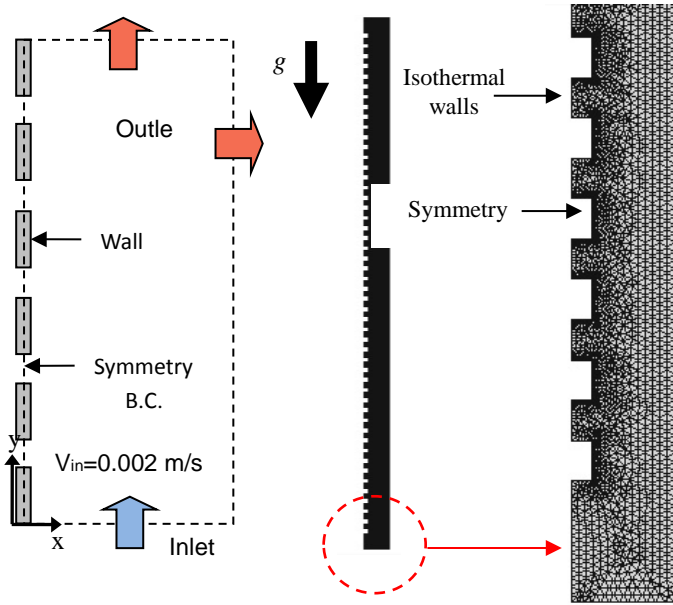


**Figure 2: a) Schematic of the numerical domain and boundary conditions for interrupted single vertical fins. b) Grid used in the model for interrupted fins.**

For solving the system of partial differential equations introduced in Section 2-1 and also for mesh generation, COMSOL software has been employed.

### 2-2 MESH INDEPENDENCY

For simulating the heat transfer in the fins a mesh was created in COMSOL Multiphysics 4.0a [14]. Three different numbers of mesh elements were used for each different geometry case and compared in terms of local temperature and total heat transfer rate to ensure a mesh independent solution. Accordingly, for the case of  $\zeta = l/t = 1$ , i.e., pin fins, and  $\gamma = G/l = 1$ , choosing a mesh number of  $2.3 \times 10^4$ , we found that the simulation of fins gives approximately 2% deviation in heat transfer rate from fins as compared to the simulation of fins with mesh number of  $5.0 \times 10^5$ . Similarly, the heat transfer rate for the simulation of fins with  $1.0 \times 10^4$  mesh elements deviate up to 9% as compared to those from the finest one. Therefore, we chose a mesh size of  $2.3 \times 10^4$  elements considering that it was sufficient for the numerical investigation purposes. A finer mesh size was applied near the fin to resolve with an enhanced accuracy the boundary layer and an increasingly coarser mesh was chosen in the middle of the domain in order to reduce the computational time.

## 3. EXPERIMENTAL STUDY

The objective of the experimental study was to investigate the effects of interruption length on the natural convective heat transfer from the rectangular vertical fins, and also to verify the results from numerical simulation explained in section 2. To

accomplish this, a custom-made testbed was designed and built, and six fin-array samples, with various geometrical parameters, were prepared. A series of tests with different surface temperatures were conducted to validate the numerical data used for calculating the Nusselt number for the vertical fins.

### 3-1 TESTBED

The testbed was designed to measure natural convective heat transfer from interrupted single fin heatsinks, as shown schematically in Fig. 3. The set-up included a metal framework from which the samples were hung, and an enclosure made of compressed foam with thickness of 20 mm to insulate the back side of the samples. It also included a power supply, two electrical heaters, which were attached to the backside of the fins base-plate, and a DAQ system. Thermal paste (Omegatherm®201) was used to minimize the thermal contact resistance between the heater and the base plate. Some of the testbed components are shown in Fig. 4.

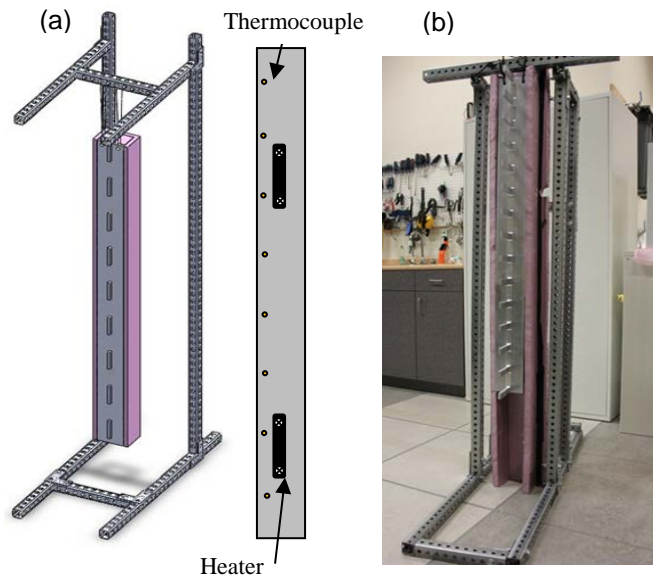


**Figure 3: a) Schematic of the single fin test-bed; b) an interrupted single fin shown in the testbed.**

Six heatsink samples with the same base plate width and different fin lengths and interruption lengths were prepared. To fully investigate the thermal boundary layer growth, different dimensions of the fins and interruptions were chosen, as listed in Table 1.

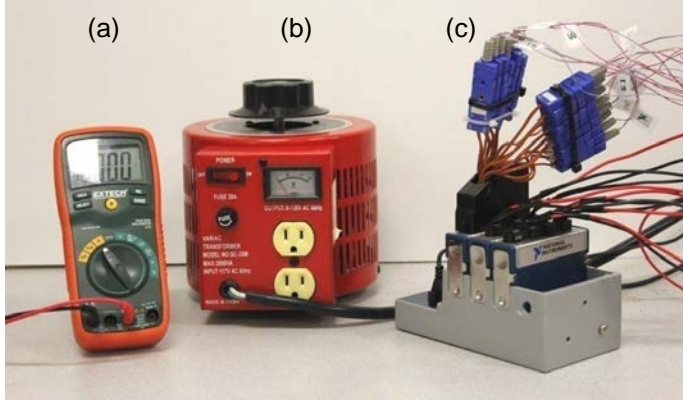


Figure 4: The tested components: a) Extech 430 multimeter, b) SC-20M Variac, c) NI 9214DAQ system.

Table 1: Dimensions of finned plate samples; interrupted fins

Sample name #	$l$ (mm)	$n$	$G$ (mm)	$L$	$G/l$	$l/t$
SW-1	50	14	50	1.45	1	5
SW-2	50	7	150	1.45	3	5
SW-3	20	17	40	1.040	2	2
SW-4	20	14	60	1.14	3	2
SW-5	10	20	30	1.452	6.2	1
SW-6	50	17	25	1.325	0.5	5

Note: Fin length base land width are constant in all the samples,  $H = 100$  mm,  $t = 10$  mm, and  $W = 101$  mm.

### 3-2 TEST PROCEDURE

The enclosures were tested in a windowless room that had an environment free of air currents. The input power supplied to the heaters and surface temperatures were measured at various locations at the back of the base-plate. Electrical power was applied using a variable voltage transformer from Variac; model SC-20M (China). The voltage and the current were measured to determine the power input to the heater. Eight self-adhesive, T-type, copper-constantan thermocouples were installed in various vertical locations on the backside surface of the aluminium samples, as shown in Fig. 3. All thermocouples were taped down to the backside surface of the enclosure to prevent disturbing the buoyancy-driven air flow. An additional thermocouple was used to measure the ambient room temperature during the experiments. Thermocouples were plugged into an NI 9214 thermocouple module supplied by National Instruments (Austin, TX). Temperature measurements were performed at eight points in order to monitor the temperature variation on the heatsink. The average of these eight readings was taken as the base plate temperature. Since the measured temperature difference between the fins and the base plate was less than  $1^\circ\text{C}$ , the fins were assumed to be at the

same temperature with the base plate. For each of the seven heatsinks, the experimental procedure was repeated for various power inputs. The base-plate temperature  $T_w$ , the ambient temperature  $T_{amb}$ , and the power input to the heater  $\dot{Q}$ , considering that the power factor equals 1, were recorded at steady-state. The steady state was considered to be achieved when the rate of temperature variations were less than  $0.1^\circ\text{C}/\text{hour}$ , which in average, was 150 minutes from the start of the experiment.

### 3-3 UNCERTAINTY ANALYSIS

Voltage (V) and current (I) were the electrical parameters measured in our experiments, from which the input power,  $P_{input}$ , can be calculated, see Eq. 7. The total accuracy in the measurements was evaluated based on the accuracy of the employed instruments in the previous sub-section. The accuracy of the voltage and current readings were 0.3% for both parameters, based on supplier's information (Extech® 430 multimeter). The reported accuracy values were given with respect to the instruments readings, and not the maximum value of the readings. The maximum uncertainty for the measurements can be obtained using the uncertainty concept provided in [15]. To calculate the uncertainty with the experimental measurements the following relation is used [15]:

$$\omega_R = \left[ \sum \left( \frac{\partial R}{\partial x_i} \omega_i \right)^2 \right]^{1/2} \quad (6)$$

where  $\omega_R$  is the uncertainty in results,  $R(x_1, x_2, \dots, x_n)$ , and  $\omega_i$  is the uncertainty of the independent variable  $x_i$ . The final form of the uncertainty for the input power becomes;

$$P_{input} = V \cdot I \quad [W], \quad (7)$$

$$\frac{\delta P_{input}}{P_{input}} = \sqrt{\left( \frac{\delta V}{V} \right)^2 + \left( \frac{\delta I}{I} \right)^2}, \quad (8)$$

$$\frac{\delta \dot{Q}_R}{\dot{Q}_R} = \sqrt{4 \left( \frac{\delta T_w}{T_w} \right)^2 + 4 \left( \frac{\delta T_{amb}}{T_{amb}} \right)^2 + \left( \frac{\delta l}{l} \right)^2 + \left( \frac{\delta H}{H} \right)^2 + \left( \frac{\delta t}{t} \right)^2}, \quad (9)$$

$$\dot{Q}_{NC} = P_{input} - \dot{Q}_R [W], \quad (10)$$

Plugging the values for  $V, I, T_w, T_{amb}, l, H$  and  $t$ , respectively, into Eqs. 8 and 9 above, the maximum uncertainty value for  $\dot{Q}_{NC}$  was calculated to be 8%. The measured temperatures uncertainty  $\Delta T$  was  $2^\circ\text{C}$ , which was twice as the accuracy of the thermocouples. The calculated uncertainties for  $\dot{Q}_{NC}$  and for  $\Delta T$  were reported as error bars in the experimental results. It should be noted that the error bars corresponding to

the power measurement uncertainty are not visible due to their relative small values as compared to the uncertainty values for the power.

#### 4. RESULTS AND DISCUSSION

We seek a solution for steady-state laminar natural convective heat transfer rate from an interrupted single fin array. A new concept called “effective fin length” is introduced to calculate the Nusselt number for the natural convective heat transfer rate along the interrupted vertical fins. The effective length is defined so that the heat transfer rate from an imaginary continuous vertical fin with this length would be equal to the heat transfer rate from the actual case, which is interrupted fin. For this purpose, the calculated heat transfer rate from the interrupted fins is made equal to the heat transfer rate from a continuous fin with effective length, and from that mathematical expression the effective length is calculated. The heat transfer from an isothermal vertical fin can be calculated from the relationship proposed in [6] :

$$Nu_{L_{eff}} = 0.59 \left( Ra_{L_{eff}} \right)^{\frac{1}{4}}, \quad (11)$$

Knowing that

$$Nu_{L_{eff}} = \frac{h L_{eff}}{k}, \quad (12)$$

Substituting  $h = \frac{\dot{Q}}{A \Delta T}$  and Eq. 12 into Eq. 11, yields:

$$L_{eff} = \left( \frac{\dot{Q}}{0.59 k} \right)^2 \left( \frac{\alpha \vartheta}{g \beta} \right)^{\frac{1}{2}} \Delta T^{-5/2}, \quad [m] \quad (13)$$

We introduce  $\zeta = l/t$ , which is a non-dimensional number equal to the ratio of the fin length  $l$ , to the fins thickness,  $t$ :

$$\zeta = l/t, \quad (14)$$

and  $\gamma$  is equal to the ratio of the interruption length,  $G$ , to the fin length,  $l$ ,

$$\gamma = G/l, \quad (15)$$

In order to develop a general model for various amounts of  $\gamma$ , two asymptotes are recognized and a blending technique [16] is implemented to develop a compact relationship for the fin effective length and the corresponding Nusselt number. The first asymptote is developed for small values of  $\gamma$ , where  $\gamma \rightarrow 0$ , for which the flow behaviour resembles the flow over a vertical plate that has no interruptions with a total length of

$$L = N.l \quad [m], \quad (16)$$

where  $N$  is the number of fins. The second asymptote is when  $\gamma \rightarrow \infty$ ; that is the limiting case where the fins are located far enough from each other, leading to an individual fin limit; in other words, the fins boundary layer will not be affected by the previous fins boundary layers. For the first asymptote,  $\gamma \rightarrow 0$ ,

$$\frac{L_{eff, \gamma \rightarrow 0}}{N.l} = 0.22\gamma + 1, \quad (17)$$

the effective length is correlated using the present numerical data.

For the asymptote  $\gamma \rightarrow \infty$ , Eqs. 19 through 21, available in literature [3, 6] are used to calculate the heat transfer from fins. Natural convective heat transfer from the fins in this asymptote is obtained by calculating the heat transfer from each side of the fin and adding them up. The relationships used for calculating the heat transfer from the upper and lower and vertical sides of the fin are given in [17] and they are the same as Eqs. 19 and 21.

$$\dot{Q}_t = \dot{Q}_{horizontal\ sides} + \dot{Q}_{vertical\ sides}, \quad [W] \quad (18)$$

$$Nu_{vertical\ sides} = Nu_l = 0.59 Ra_t^{\frac{1}{4}}, \quad (19)$$

$$Nu_{horizontal\ sides} = Nu_{up} = 0.56 Ra_t^{\frac{1}{4}}, \quad (20)$$

$$Nu_{low} = 0.27 Ra_t^{\frac{1}{4}}, \quad (21)$$

The natural convective heat transfer,  $\dot{Q}$ , as calculated from the equations above, could be substituted in Eq. 13 in order to calculate the asymptote of  $L_{eff}$  for larger values of  $\gamma$ ,  $L_{eff, \gamma \rightarrow \infty}$ . As a result, for the upper, lower and vertical sides of the fins, we can calculate the ratio of the effective length to  $N.l$  as:

$$\frac{L_{eff, \gamma \rightarrow \infty}}{N.l} = N^{\frac{1}{3}} \left[ 0.83 \left( \frac{1}{\zeta} \right)^{\frac{3}{4}} + 1 \right]^{4/3}, \quad (22)$$

Having  $L_{eff, \gamma \rightarrow \infty}$  and  $L_{eff, \gamma \rightarrow 0}$  available, a compact relationship for  $L_{eff}$  can be developed by using a blending technique, introduced by Churchill and Usagi [16].

where  $c$  is a fitting parameter, and its value is found by

$$L_{eff} = \left[ (L_{eff, \gamma \rightarrow 0})^{-c} + (L_{eff, \gamma \rightarrow \infty})^{-c} \right]^{-1/c}, \quad [m], \quad (23)$$

comparison with the present numerical data to be  $c = 3$ . This fitting parameter minimizes the maximum percent difference between the model and the exact solution, as it is shown in the comparison showed in Fig. 4-8.

$Nu_{L_{eff}}$  is calculated by substituting  $L_{eff}$  into Eq. 12. The final relationship is a function of  $\gamma$ ,  $\zeta$ ,  $N$  and Rayleigh number, which in turn, is a function of temperature difference, as shown below:

$$Nu_{L_{eff}} = \frac{h L_{eff}}{k} = 0.59 Ra_t^{1/4} N^{3/4} \left\{ (0.22\gamma + 1)^{-3} + \left[ N \left( 0.83 \left( \frac{1}{\zeta} \right)^{\frac{3}{4}} + 1 \right)^4 \right]^{-1} \right\}^{-1/4} \quad (24)$$

where  $l$  is the fin length,  $\zeta$  is the aspect ratio of the fin length of the fin thickness,  $\zeta = l/t$ ,  $\gamma$  is the ratio of the interruption length to the fin length,  $\gamma = G/l$ .  $N$  is the number of fins and  $Ra_l$  is the Rayleigh number based on fin length, respectively.

$L_{eff}$  is the effective length for the fins, the relationship proposed for  $Nu_{L_{eff}}$  is valid for the following range: ( $5 < \zeta = \frac{l}{t} < 15$ ).

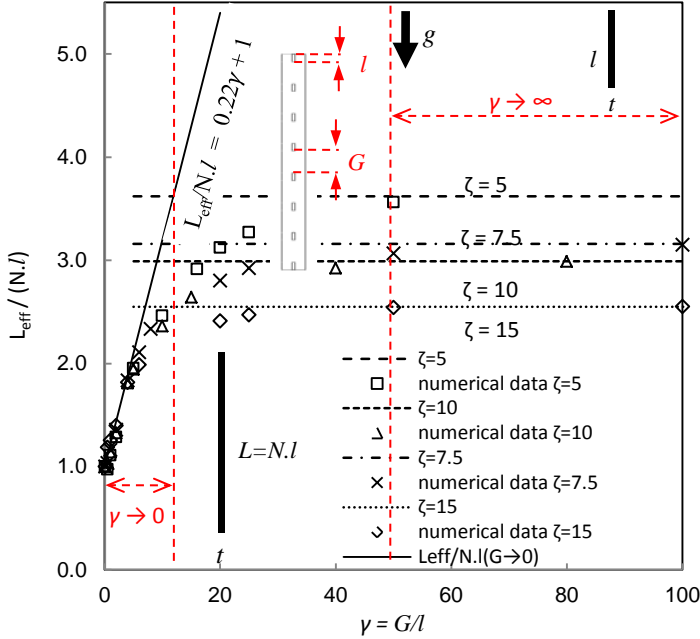


**Figure 5: Numerical data and asymptotes for natural convective heat transfer from interrupted fins.**

Figure 5 highlights the tendencies that the two asymptotes, exhibit based on  $\gamma$ . Two different trends can be seen in the present data for the extreme values of  $\gamma$ , where  $\gamma$  is the ratio of the interruption length to the fin length,  $\gamma = G/l$ . The first trend is showing small values of  $\gamma$  and it can be seen that the data in this region have been collapsed to the same value as shown in Fig. 6. The second trend of data, which corresponds to relatively large values of  $\gamma$ , shows a plateau. i.e., data converge to a specific value, which is the asymptote for fins with effective length equal to the fin length ( $L_{eff} = l$ ).

A new compact relationship, Eq. 25, is developed to determine the Nusselt number that characterizes the natural heat transfer from interrupted fins. The calculation is performed using a blending technique [16] based on the non-dimensional geometrical parameters  $\gamma = G/l$  and  $\zeta = l/t$ . This Nusselt number can be used to calculate the heat transfer rate for any rectangular interrupted fin in the range of  $5 < \zeta = l/t < 15$ .

$$Nu_{L_{eff}} = 0.59 Ra_l^{1/4} N^{3/4} \left\{ (0.22\gamma + 1)^{-3} + \left[ N \left( 0.83 \left( \frac{1}{\zeta} \right)^{3/4} + 1 \right) \right]^{-1} \right\}^{-1/4}, \quad (25)$$

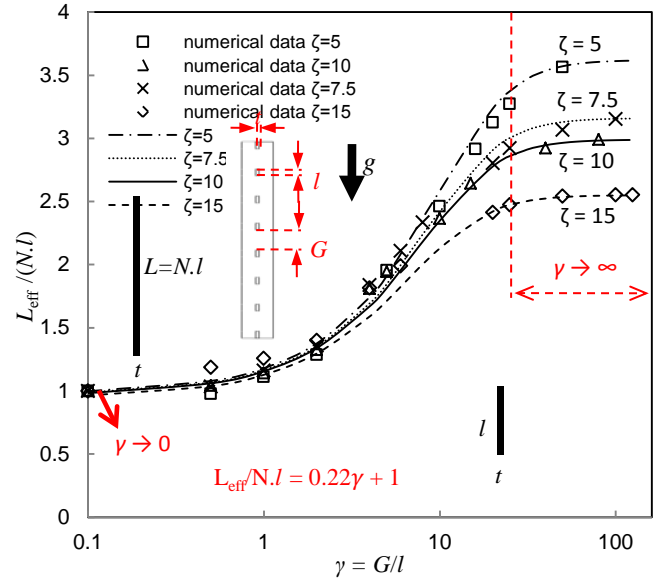


**Figure 6: Numerical data and analytical relationship - natural convective heat transfer from interrupted fins.**

where  $l$  is the fin length,  $\zeta$  is the aspect ratio of the fin length of the fin thickness,  $\zeta = l/t$ ,  $\gamma$  is the ratio of the interruption length to the fin length,  $\gamma = G/l$ .  $N$  is the number of fins and  $Ra_l$  is the Rayleigh number based on fin length, respectively. Experimental data obtained from interrupted wall samples is compared against Eq. 25 in Fig. 7. It should be noted that out of six samples tested, three of them could not be used since their fin aspect ratios were out of the applicable range of the proposed Eq. 25.

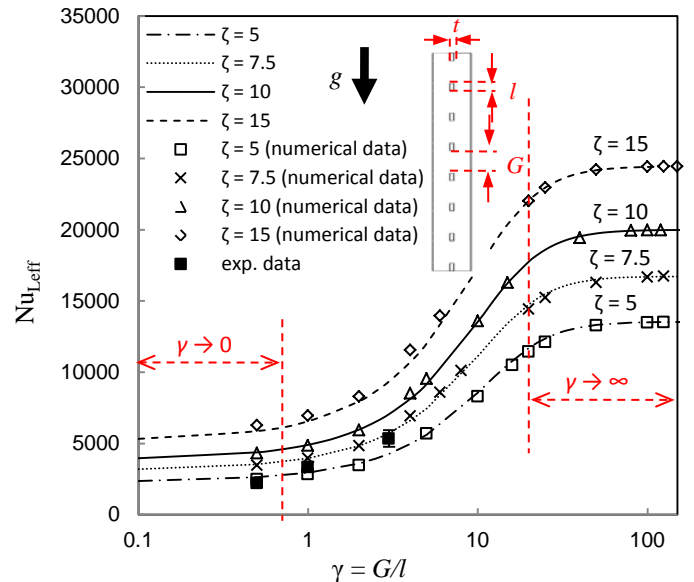


**Figure 7: Comparison between the present numerical data and the proposed compact relationship for Nusselt number of interrupted fins. ( $\zeta = l/t$ )**

## 5. CONCLUSION

• Experimental, numerical and analytical studies were performed in order to establish a compact correlation for natural convective heat transfer from vertically-installed interrupted rectangular fins. A new custom-designed testbed was developed and six fin array and interrupted fin samples were prepared to verify the developed numerical and analytical models over the entire range of fin parameters. The prepared samples were tested in the lab and collected data were compared with the numerical and analytical models developed in this study. The numerical and analytical results were successfully verified by experimental data; the mean relative difference found was 22% and the maximum relative difference was 36%.

• The most important element of the present work is the determination of the effect of interruption length in natural convection fin arrays. The purpose of these interruptions is to reset the thermal boundary layer associated with the fin in order to decrease thermal resistance.

• The following can be considered as the study's highlight:

A new compact relationship is developed for the Nusselt number for natural convective heat transfer from interrupted fins using a blending technique based on the non-dimensional geometrical parameters  $\gamma = G/l$  and  $\zeta = l/t$ . This relationship can be used for calculating heat transfer rate for any rectangular interrupted fin in the range of  $5 < \zeta = \frac{l}{t} < 15$ .

$$Nu_{L_{eff}} = 0.59 Ra_t^{1/4} N^{3/4} \left\{ (0.22\gamma + 1)^{-3} + \left[ N \left( 0.83 \left( \frac{1}{\zeta} \right)^{3/4} + 1 \right)^4 \right]^{-1} \right\}^{-1/4}$$

## NOMENCLATURE

$A$	Surface area, m <sup>2</sup>
$g$	Gravitational acceleration, m <sup>2</sup> /s
$G$	Fin interruption length, m
$Gr$	Grashof number
$h$	Convection heat transfer coef. W/m <sup>2</sup> K
$I$	Electrical current, A
$k$	Thermal conductivity, W/m K
$l$	Fin length, m

$L$	Total length of fins, m
$L_{eff}$	Effective length, m
$n$	Number of interruptions
$N$	Number of fins per row
$Nu$	Nusselt number
$P_{input}$	Input power, W
$Pr$	Prandtl number
$\dot{Q}$	Heat transfer rate, W
$Ra$	Rayleigh number
$t$	Fin thickness, m
$T$	Temperature, K
$u$	Flow velocity in x direction, m/s
$v$	Flow velocity in y direction, m/s
$V$	Electrical voltage, V
$W$	Enclosure width, m
$x$	Direction normal to fin surface, m
$y$	Direction along fin surface, m

## Greek symbols

$\alpha$	thermal diffusivity
$\beta$	Coefficient of volume expansion, 1/K
$\gamma$	Interruption length to wall length ratio
$\zeta$	Wall length to wall thickness ratio
$\mu$	Fluid viscosity, Ns/m <sup>2</sup>
$\rho$	Density, kg/m <sup>3</sup>

## Subscripts

atm	Atmosphere
NC	Natural convection
R	Radiation
s	surface
up	Upper side of the fin/wall

**REFERENCES**

[1] S. P. Gurrum, S. K. Suman and J. Y. K., " Thermal issues in next-generation integrated circuits," *IEEE Transactions on device and materials reliability*, vol. 4, no. 4, pp. 709-714, 2004.

[2] R. Chu and R. Simons, "Recent development of computer cooling technology," *International symposium on transport phenomena in thermal engineering*, vol. 5, pp. 17-25, 1993.

[3] H. Yuncu and G. Anbar, "An experimental investigation on performance of fins on a horizontal base in free convection heat transfer," *Journal of heat and mass transfer*, vol. 33, no. 5-6, pp. 507-514, 1998.

[4] B. Yazicioglu and H. Yuncu, "Optimum fin spacing of rectangular fins on a vertical base in free convection heat transfer," *Journal of heat and mass transfer*, vol. 44, no. 1, pp. 11-21, 2007.

[5] F. Harahap and H. McManus, "Natural convection heat transfer from horizontal rectangular fin arrays," *Journal of heat transfer*, vol. 89, no. 1, pp. 32-39, 1967.

[6] S. Ostrach, "An analysis of free convection flow and heat transfer about a flat plate parallel to the direction of the generating of the body force," NACA, 1953.

[7] E. Sparrow and J. L. Gregg, "Laminar free convection from a vertical flat plate," *ASME*, vol. 80, pp. 435-440 , 1956.

[8] S. Churchill and H. Chu, "Correlating equations for laminar and turbulent free convection from a vertical plate," *International journal of heat and mass transfer*, vol. 18, no. 11, pp. 1323-1329, 1975.

[9] A. Daloglu and T. Ayhan, "Natural convection in a periodically finned vertical channel," *International Communications in Heat and Mass Transfer*, vol. 26, no. 8, p. 1175-1182, 1999.

[10] S. Nada, "Natural convection heat transfer in horizontal and vertical closed narrow enclosures with heated rectangular finned base plate," vol. 50, 2007.

[11] A. Nakhi and A. Chamkha, "Conjugate natural convection in a square enclosure with inclined thin fin of arbitrary length," *International journal of thermal sciences*, vol. 46, no. 5, p. 467-478, 2007.

[12] M. Fujii, "Enhancement of natural convection heat transfer from a vertical heated plate using inclined fins," *Heat Transfer—Asian Research*, vol. 36, no. 6, pp. 334-344, 2007.

[13] A. Bejan, *Convection heat transfer*, Prentice Hall, 1984.

[14] *COMSOL Multiphysics Finite Element Analysis Software (4.2)*.

[15] J. P. Holman, *Experimental Methods for Engineering*, 7th ed., New York: McGrawHill, 2001.

[16] S. W. Churchill and R. Usagi, " A general expression for the correlation of rates of transfer and other phenomenon," *AICHE*, vol. 18, no. 6, p. 1121-1128, 1972.

[17] R. J. Goldstein, E. M. Sparrow and D. C. Jones, "Natural convection mass transfer adjacent to horizontal plates," *Int. journal of heat mass transfer*, vol. 16, pp. 1025-1035, 1973.

[18] R. Remsburg, *Advanced Thermal Design of Electronic Equipment*, Chapman & Hall, 1998.

[19] Available at: [www.bccresearch.com/report/thermal-management-technologies-market..](http://www.bccresearch.com/report/thermal-management-technologies-market..)

[20] A. Daloglu and T. Ayhan, "Natural convection in a periodically finned vertical channel," *International Communications in Heat and Mass Transfer*, vol. 26, no. 8, p. 1175-1182, 1999.

[21] A.B.-Nakhi and A. Chamkha, "Conjugate natural convection in a square enclosure with inclined thin fin of arbitrary length," vol. 46, 2007.

[22] A. Daloglu and T. Ayhan, "Natural convection in a periodically finned vertical channel," *International Communications in Heat and Mass Transfer*, vol. 26, no. 8, p. 1175-1182, 1999.